Formation of β-Fluoroethyl Radical and Closed-Shell Products in Reactions of Photogenerated Fluorine Atoms with Ethene in Solid Argon

3 AUTHORS:

Eugenii Ya Misochko
Russian Academy of Sciences
65 PUBLICATIONS **519** CITATIONS

SEE PROFILE

Alexander Benderskii
University of Southern California
36 PUBLICATIONS **885** CITATIONS

SEE PROFILE

Charles A. Wight
Weber State University
140 PUBLICATIONS **3,583** CITATIONS

SEE PROFILE

Formation of β-Fluoroethyl Radical and Closed-Shell Products in Reactions of Photogenerated Fluorine Atoms with Ethene in Solid Argon

Eugenii Ya. Misochko,[†] Alexander V. Benderskii, and Charles A. Wight*

Department of Chemistry, University of Utah, Salt Lake City, Utah 84112

Received: October 26, 1995; In Final Form: December 14, 1995[⊗]

Solid-state reactions of F atoms with ethene molecules were initiated by UV photolysis of dilute solutions of F_2 and C_2H_4 in solid Ar. Products stabilized in the matrix were detected by infrared spectroscopy. Experiments were conducted at different temperatures in order to distinguish reactions in matrix-isolated F_2-C_2H_4 complexes (at 16 K) from reactions of diffusing thermal F atoms (at 26 K). Comparison with the kinetic EPR data (Benderskii, V. A. *et al. Mendeleev Commun.* **1995,** *6*, 245) permitted the identification of the infrared spectrum of the β-fluoroethyl radical, which is the main product of the F + C_2H_4 reaction. Frequencies and absolute absorption intensities of the eight strongest infrared bands of β-C_2H_4F are reported. Photolysis of isolated F_2-C_2H_4 complexes forms the closed-shell products C_2H_3F−HF and *trans*- and *gauche*-1,2-$C_2H_4F_2$ with relative yields 0.6:0.2:0.2. Successive addition of two thermal F atoms to an isolated C_2H_4 molecule forms only the two conformers of 1,2-$C_2H_4F_2$. The difference between product branching ratios of the latter reaction and the direct photoinduced reaction of F_2−C_2H_4 complexes is qualitatively explained by the difference in size of the reaction cages and excess energies of the vibrationally excited intermediate $(C_2H_4F_2)^*$.

INTRODUCTION

Studies of the photodissociation of F_2 molecules isolated in rare gas solids by Apkarian and co-workers[1−4] revealed some important characteristics about the mobility of the photoproduced F atoms. Two mechanisms can be distinguished. Translationally "hot" F atoms that are formed by photodissociation of F_2 with excess translational energy of more than 1 eV escape from the parent precursor cage and can undergo long-range migration through the Ar lattice (over distances on the order of 100 Å). Thermalized F atoms are immobilized in the lattice at $T < 20$ K but are able to diffuse over similar distances at 22−26 K on a time scale of 10^4-10^3 s. These features of F atom mobility in low-temperature rare gas solids form a basis for further investigations of the mechanisms of their solid-state chemical reactions. Our first results of such studies in solid F_2−CH_4−Ar and F_2−C_2H_4−Ar mixtures using EPR methods were reported recently.[5−7] The present paper, which is a continuation and extension of the EPR study[7] (hereafter referred to as I), is devoted to experimental investigation of reactions of hot and thermalized F atoms with C_2H_4 molecules in solid Ar by FTIR spectroscopy.

Gas-phase reactions of F atoms with C_2H_4 molecules were extensively investigated as an example of the reactive collision dynamics[8−12] and also as an important step in the chain reactions in fluorine−ethene mixtures.[13] The dominant reaction channel begins with formation of the β-fluoroethyl radical (CH_2CH_2F) intermediate with about 50 kcal/mol of excess energy:

$$F + C_2H_4 \rightarrow C_2H_4F \qquad (1)$$
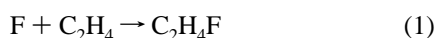
This energy-enriched adduct decomposes on the time scale of 10^{-9} s, forming vinyl fluoride and an H atom. Another important channel is hydrogen atom abstraction which produces vinyl radical

$$F + C_2H_4 \rightarrow C_2H_3 + HF \qquad (2)$$
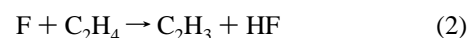
The products of the reaction between F atoms produced in a microwave discharge and ethene were trapped in an Ar matrix and investigated using IR spectroscopy in an early experimental study by Jacox.[14] Formation of both primary (β-fluoroethyl radical) and secondary products (C_2H_3F, HF, and $C_2H_4F_2$ molecules) was inferred from the IR spectrum of the solid deposit.

Reactions in matrix-isolated F_2−C_2H_4 complexes induced by IR excitation of ethene vibrational modes were studied by Hauge *et al.*[15] and Frei *et al.*[16,17] One-photon absorption leads to formation of the C_2H_3F−HF complex and *trans*- and *gauche*-1,2-$C_2H_4F_2$ as major products. The results were explained in terms of a reaction mechanism in which addition of F_2 across the double bond of ethene leads to the formation of vibrationally excited $(C_2H_4F_2)^*$, which subsequently decomposes into C_2H_3F and HF or undergoes vibrational relaxation forming the conformers of 1,2-$C_2H_4F_2$.

In our previous study I, reactions of F atoms with ethene in triple mixtures (Ar−F_2−C_2H_4) were investigated using EPR spectroscopy upon UV photolysis of F_2. The principal results were as follows:

(1) At 13 K, the product of the reactions of the hot F atoms with C_2H_4 molecules is β-fluoroethyl radical (reaction 1).

(2) No evidence for vinyl radical was found in the EPR spectra of the photolyzed samples.

(3) A 6−10-fold increase of the β-C_2H_4F radical concentration was observed when samples photolyzed at 13 K were annealed to 26 K. This increase was attributed to thermally induced diffusion of the F atoms participating in reaction 1.

(4) The estimated rate constant for reaction 1 of the thermalized F atoms at 20 K is $k_1 \approx 10^{-24}$ cm^{-3} s^{-1}, which is an order of magnitude smaller than the diffusion limit at this temperature but 2−3 orders of magnitude higher than the rate constant for H atom abstraction from CH_4 under analogous experimental conditions.[5]

There are two possible scenarios for stabilization of C_2H_4F radicals at $T < 20$ K. The first of these involves photolysis of

Reactions of Photogenerated F Atoms with Ethene

J. Phys. Chem., Vol. 100, No. 11, 1996 **4497**

a matrix-isolated complex, $C_2H_4-F_2$, in which one of the nascent F atoms escapes from the lattice cage, thereby preventing its recombination with the radical. In the second, the two reactants are initially separated, and one of the translationally hot F atoms formed from photolysis of F_2 must find the C_2H_4 reaction partner before it thermalizes and is trapped in the lattice. The possibility that such hot F atoms can react by undergoing long-range migration was established earlier in experiments on photolysis of F_2 molecules in solid methane.[18] Using the EPR method it was shown that methyl radical pairs $CH_3\cdots CH_3$ are formed in which the intrapair separation distance is 9−20 Å. Complementary experiments using infrared detection revealed that closed-shell products are formed as well, via the cage reaction

$$[F + F + CH_4] \rightarrow [CH_3F + HF] \qquad (3)$$

Reaction yields of the closed-shell products via (3) and radical pairs are about 1:1.

Earlier, Johnson and Andrews[19] showed that F_2 photolysis in $Ar-F_2-CH_4$ mixtures at 14 K yields predominantly closed-shell reaction products (3). Methyl radicals are formed in concentrations detectable by IR spectroscopy only upon annealing to 24−25 K due to reactions of thermally mobilized atoms. These results imply that the photolysis of F_2 in matrix-isolated complexes with the reaction partner does not necessarily lead to the cage escape by one of the nascent atoms, as is the case for the photolysis of single isolated fluorine molecules.[1]

In the present work our goal is to establish the main reaction channels of hot and thermalized F atoms with C_2H_4 in solid Ar using IR spectroscopy and to compare the results with the previous EPR study I. The combination of experimental results obtained by these two complementary methods allows unambiguous identification of both the closed-shell products of the reaction and radical intermediates stabilized in the inert matrix. Studies carried out at temperatures in the range 13−30 K have permitted us to distinguish between three different reaction modes: photolysis of $F_2-C_2H_4$ matrix-isolated complexes, reaction of single translationally hot F atoms at $T < 20$ K, and reaction of thermalized F atoms by diffusion at higher temperatures.

EXPERIMENTAL SECTION

Matrix samples were prepared by vapor deposition onto a surface of a CsI window held at a base temperature of 16 K by means of a closed-cycle helium refrigerator (APD Cryogenics model). For experiments conducted at higher temperatures, a temperature controller (Lakeshore Cryotronics Model 330) was used to maintain the desired substrate temperature to within 0.05 K by means of a resistance wire heater wound around the cold tip of the refrigerator.

Ethene (Aldrich, 99.5+%) was purified by freezing at liquid nitrogen temperature and pumping out more volatile impurities. Fluorine (Spectra Gases, 10% in Ar) was used without further purification. Argon (Spectra Gases, 99.999%) was used for the matrix material without further purification. In order to minimize reaction in the gas phase, mixtures of F_2-Ar and C_2H_4-Ar were prepared in separate manifolds. Deposition lines from the two manifolds merge before entering the vacuum chamber housing the cryostat. The fluorine manifold and deposition lines are made of stainless steel and were passivated with fluorine prior to each experiment. Gas flow rates from the two channels were adjusted throughout the deposition process by means of two needle valves to maintain the desired $F_2:C_2H_4$ ratio in the sample. Deposition rates were typically 70 μmol/min. The area of the sample was approximately 5 cm^2.

A total of 5−10 μmol of each reactant was deposited, along with different amounts of Ar (5−15 mmol), depending on the dilution degree (typically, 1:1:1000 mixtures were used in this study). IR spectra were recorded at 0.5 and 0.25 cm^{-1} resolution by a Mattson Model RS/1000 FTIR spectrometer.

Photolysis of the samples was performed by pulsed 355 nm light from the third harmonic of a Nd:YAG laser (Continuum Model Surelite). The repetition frequency is 10 Hz. Photodissociation of an F_2 molecule at this wavelength produces two F atoms with ~1 eV translational energy each. The central part of the laser beam is selected by an iris and expanded by a quartz lens to exceed the area of the sample probed by the IR spectrometer. The average laser power was 10 mW/cm^2. Experiments at lower photolysis intensity (1 mW/cm^2) were conducted to rule out the possibility of nonlinear absorption processes. No significant changes were observed in the IR spectra of samples left in the dark at 16 K or exposed to the IR source of the spectrometer.

The following impurities were found in the IR spectra of deposited samples: CO_2 (661.9, 2340.5 cm^{-1}), OF_2 (825.7 cm^{-1}), NF_2 (932.2 cm^{-1}), F_2CO (965.2, 1237.9 cm^{-1}), and FCO (1022.9 cm^{-1}). The intensities of these bands do not change upon photolysis or annealing. A line assigned to FO_2 (1489.0 cm^{-1}) appears in the spectra of photolyzed samples at 20−25 K. Oxygen is a common impurity in fluorine gas and is difficult to remove by fractional distillation. Products of prereaction in the deposition lines are mainly matrix-isolated HF (doublet 3953.6 and 3961.9 cm^{-1})[20] and vinyl fluoride (1148.6 cm^{-1}), which are present in the samples after deposition.

RESULTS

A. Photolysis at 16 K. Laser photolysis of samples at 16 K leads to the appearance of intense bands in the regions of C−F and H−F stretching vibrations. IR spectra demonstrating the growth of the bands in the C−F stretching region are shown in Figure 1A. These features have been definitively identified by several authors[21,22,14−16] as *trans*-1,2-$C_2H_4F_2$ (1047.5 cm^{-1}, $\nu(C-F)$, B_u), *gauche*-1,2-$C_2H_4F_2$ (1070.3 and 1096.0 cm^{-1}, $\nu(C-F)$, B, and $\nu(C-F)$, A, respectively), and C_2H_3F (1122.4 cm^{-1}, ν_7) in complex with HF (3801.8 cm^{-1}). Other bands of these molecules also appear in the IR spectra. The appearance of two broad bands with maxima at 1139 and 1087 cm^{-1} can also be noticed in Figure 1A. The spectrum of the ν_7 vibrational mode of C_2H_4 and its changes in the course of photolysis are shown in Figure 2. The maximum of the ν_7 band of ethene molecules consumed in photolysis is shifted by ~1 cm^{-1} to higher frequencies from the maximum of the pure matrix-isolated ethene band (947.3 cm^{-1}) observed in control experiments. Comparison of the C_2H_4 spectrum in samples with and without fluorine ($F_2-C_2H_4-Ar = 1:1:1000$ and $C_2H_4-Ar = 1:1000$) shows a small shift of the maximum of the ν_7 band and the appearance of a weak shoulder on the high-frequency side (Figure 2A). Subtraction of the spectra normalized by the total amount of ethene in the samples gives a band with a maximum at 948.2 cm^{-1}, whose appearance corresponds to formation of $F_2-C_2H_4$ complexes. The fraction of these complexes in the spectrum of a 1:1:1000 sample is 0.04−0.08, increasing to 0.10−0.15 in a 2:1:1000 sample. Formation of molecular complexes is common in matrix-isolated halogen-olefin systems, with shifts of the olefin vibrational bands from 1 to 10 cm^{-1}.[23,16,24] At 16 K, photolysis decreases the concentration of $F_2-C_2H_4$ complexes, but there is little decrease in concentration of isolated ethene molecules (~0.05−0.1 of the total ethene consumption), as can be seen in Figure 2B.

Experiments conducted at different photolysis light intensities and fluorine concentrations demonstrated that the band intensi-
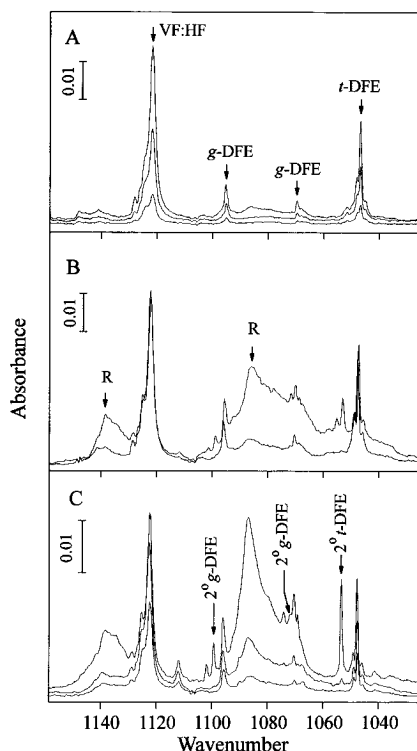
Figure 1. Growth of the product absorptions in the infrared spectra of the Ar−F_2−C_2H_4 mixtures (CF stretch region): (A) during 355 nm photolysis at 16 K, after 1, 4, and 40 min; the primary products (see text) are indicated by arrows; (B) upon annealing to 20 K (lower spectrum), 28 K; (C) during photolysis at 26 K, after 10 min, 50 min, and 9 h. Secondary products are indicated (see text). Initial spectra of the samples (before photolysis), containing impurities and products of prereaction in the deposition line, have been subtracted.
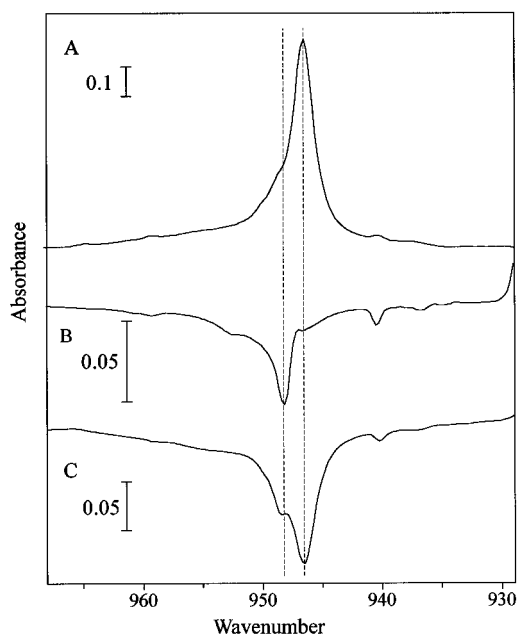

Figure 2. (A) ν_7 of ethene band in 1:1:1000 F_2−C_2H_4−Ar mixture. (B) Difference spectrum of ethene consumption during photolysis at 16 K. (C) Difference spectrum of ethene consumption during photolysis at 26 K.

ties of the products listed above are proportional to the total dose of irradiation and the F_2 concentration during the initial stage of photolysis. This shows that the reactions are initiated by one-photon light absorption by F_2 molecules.

Figure 3 presents the kinetics of the closed-shell products C_2H_3F−HF, *trans*-$C_2H_4F_2$, and *gauche*-$C_2H_4F_2$ during photolysis. It is obvious that the absorption bands of these species
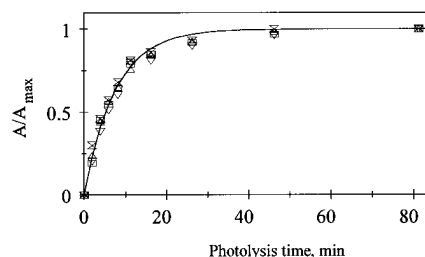
Figure 3. Photokinetic curves of the absorption bands of the photolysis products: HF−C_2H_3F complex at 3801.8 (∇) and 1122.4 cm^{-1} ($\triangle$), *trans*-1,2-$C_2H_4F_2$ at 1047.5 cm^{-1} ($\boxtimes$), and *gauche*-1,2-$C_2H_4F_2$ at 1096.0 cm^{-1} ($\square$). The integrated absorbance of each band has been normalized by its value after 80 min of photolysis. The solid curve is a single exponential fit.
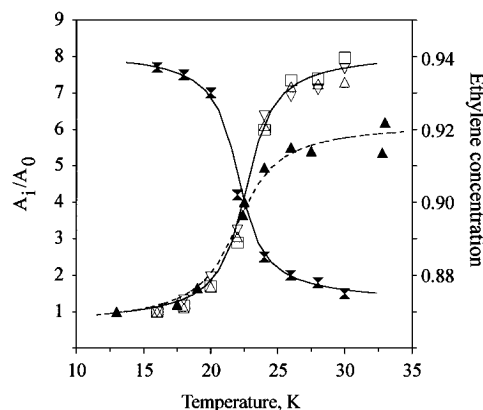

Figure 4. Growth of the product bands at 1139 (∇), 1087 ($\triangle$), and 1449 cm^{-1} ($\square$) during warming of a 1:1:1000 F_2−C_2H_4−Ar sample photolyzed at 16 K. The integrated absorbance of each band has been normalized by its value at the initial temperature (left side axis). For comparison, the growth of β-fluoroethyl radical concentration ($\blacktriangle$), measured in I by EPR under similar experimental conditions, is shown. Product growth is accompanied by a diminution of the ethene ν_7 band ($\mathbf{Ɪ}$, right side axis).

grow simultaneously (their relative intensities are constant) and reach a saturation limit after extended photolysis periods. The decrease in ethene concentration obeys the same kinetics. The saturation limit corresponds to consumption of ∼6% of the C_2H_4 in standard 1:1:1000 samples resulting from the complete bleaching of the F_2−C_2H_4 complexes.

B. Annealing of Samples Photolyzed at 16 K. IR spectra of samples photolyzed at 16 K do not clearly show bands that can be attributed to the β-fluoroethyl radicals, whose formation under similar conditions was observed in the EPR study I. We annealed samples photolyzed at 16 K with the purpose of increasing the concentration of the radicals. The samples were photolyzed until the saturation limit of the C_2H_3F and $C_2H_4F_2$ bands was reached. Evolution of the spectra upon annealing is shown in Figure 1B.

The bands corresponding to the closed-shell products of 16 K photolysis are unchanged upon warming to 28 K. On the other hand, fast growth of the broad bands at 1087 and 1139 cm^{-1} as well as other bands (see next subsection) occurs at T ≥20 K. This growth is accompanied by consumption of ethene in the sample. The relative decrease in C_2H_4 concentration is ∼0.1 in standard 1:1:1000 samples.

Growth of the 1087, 1139, and 1449 cm^{-1} bands during warming at a constant rate (∼0.2 K/min) is shown in Figure 4 along with the decrease in concentration of C_2H_4 molecules. Also shown are growth of concentration of β-C_2H_4F radicals measured by EPR in I at the same warming rate. There is obvious correlation between increase of intensity of these bands, consumption of ethene molecules, and growth of radical concentration at temperatures 22−28 K. According to the

Reactions of Photogenerated F Atoms with Ethene

J. Phys. Chem., Vol. 100, No. 11, 1996 **4499**
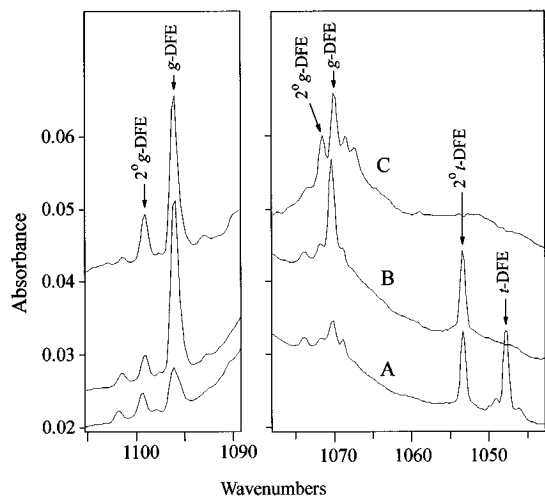
Figure 5. Changes in the spectrum of *trans*- and *gauche*-1,2-difluoroethane, obtained by photolysis of a 1:1:1000 $F_2-C_2H_4-Ar$ sample at 26 K (A), and upon annealing to 30 K for 3 h (B) and, subsequently, to 34 K for 70 h (C).

experimental data of Apkarian and co-workers,[1] it is this temperature range where F atoms, photogenerated at 10 K in solid Ar, undergo thermally induced recombination upon warming of the sample at similar rates.

Annealing of the samples to yet higher temperature results in interconversion of the bands corresponding to *trans*- and *gauche*-1,2-$C_2H_4F_2$ formed by 16 K photolysis (see Figure 5). At 30 K, the 1047.5 cm^{-1} band disappears entirely, and a corresponding increase in the 1096.0 and 1070.3 cm^{-1} bands is observed. Similar conversion of *trans*-difluoroethane to the more stable *gauche* form was observed by Gunthard and co-workers at $T \geq 30$ K for 1,2-difluoroethane molecules isolated in an Ar matrix.[25]

C. Photolysis at 26 K. Evolution of the IR spectrum of a 1:1:1000 sample upon photolysis at 26 K is presented in Figure 1C. The kinetics of the bands corresponding to C_2H_3F-HF complexes and *trans*- and *gauche*-1,2-$C_2H_4F_2$ are similar to those at 16 K (see Figure 6). The broad bands at 1087 and 1139 cm^{-1} have different kinetics, as can be seen from Figure 6. Growth of these bands is 5-10 times faster than at 16 K photolysis. Similarly, the quantum yield of β-C_2H_4F radicals measured in I increases by a factor of 6-10 for the photolysis at 26 K compared to 13 K.

Analysis of the ethene consumption spectra (Figure 2C) shows that two components of the ν_7 band of ethene (corresponding to isolated C_2H_4 and $F_2-C_2H_4$ complexes) are consumed by 26 K photolysis. Consumption of the complexes correlates well with production of $C_2H_4F_2$ and C_2H_3F-HF, whereas consumption of the isolated ethene molecules coincides with growth of the broad bands.

Extended photolysis of the samples leads to appearance of new narrow absorption bands at 1053.2, 1073.9, and 1099.2 cm^{-1}. These are shifted by 5-8 cm^{-1} to higher frequencies from the 1047.5, 1070.3, and 1096.0 cm^{-1} bands of *trans*- and *gauche*-1,2-$C_2H_4F_2$ formed by reaction in complexes. Growth kinetics of the strongest band, assigned to *trans*-1,2-$C_2H_4F_2$ (1053.2 cm^{-1}), is shown in Figure 6. The kinetic curve for this band has zero initial slope and a characteristic sigmoidal shape. This implies that this band corresponds to a secondary product, and absorption of two photons is required for its formation. On the basis of the fact that the new bands are close to those of the primary products *trans*- and *gauche*-1,2-$C_2H_4F_2$, we suggest that they are also due to these molecules but are stabilized in a different matrix environment. As can be seen from Figure 1C, the intensity of the secondary *trans*-1,2-$C_2H_4F_2$
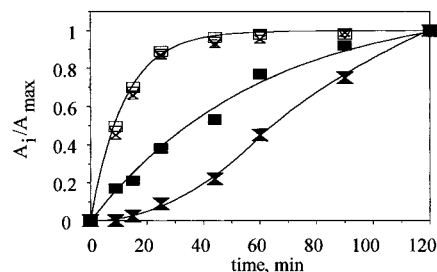
Figure 6. Growth of the product absorptions upon photolysis at 26 K: C_2H_3F-HF (∇), *trans*-1,2-$C_2H_4F_2$ ($\nabla\triangle$), *gauche*-1,2-$C_2H_4F_2$ ($\square$), β-fluoroethyl radical ($\blacksquare$), and secondary *trans*-1,2-$C_2H_4F_2$ ($\mathbf{I}$), 1053.2 cm^{-1} band. Each band is normalized by its absorption intensity after 120 min of photolysis.

TABLE 1: Characteristics of Infrared Absorption Bands for C_2H_4, C_2H_3F, and *trans*- and *gauche*-1,2-$C_2H_4F_2$ Trapped in Solid Ar at 16 K

ν, cm^{-1}	species	vibration	integrated absorption cross section B_i, km/mol[a]
947.3	C_2H_4	ν_7	93
1440.3	C_2H_4	ν_{12}	12.5
1148.6	C_2H_3F	ν_7, $\delta(C-F)$	37.4
1650.0	C_2H_3F	ν_4, $\delta(C=C)$	37.1
1047.5	t-$C_2H_4F_2$	$\nu(C-F)$, B_u	31.1
1096.0	g-$C_2H_4F_2$	$\nu(C-F)$, A	9.1

[a] Base e.

(1053.2 cm^{-1}) exceeds that of the primary *trans*-1,2-$C_2H_4F_2$ (1047.5 cm^{-1}) after extended photolysis. However, no new features appear in the region of vinyl fluoride (1100-1150 cm^{-1}) and HF (3500-4000 cm^{-1}). The new bands of secondary difluoroethane also show *trans*-*gauche* interconversion upon annealing (Figure 5). However, this requires higher temperatures than interconversion of the primary difluoroethane; the characteristic interconversion rate of the secondary product at 30 K is at least 2 orders of magnitude slower.

D. Measurements of IR Absorption Intensities of Ethene and Products. In order to measure the yields of the products and compare them with consumption of ethene, we performed calibration experiments to determine absolute IR absorption intensities of C_2H_4 and C_2H_3F molecules isolated in an Ar matrix by a method described in detail elsewhere.[24] In order to determine the absolute absorption intensities of *trans*- and *gauche*-1,2-difluoroethane from that of vinyl fluoride, we used the ratios of the absorption intensities of these molecules isolated in matrix measured by Frei *et al.*[16] Additionally, we employed the relative change in band intensities of *trans*- and *gauche*-1,2-difluoroethane during their interconversion upon annealing to determine the ratio of their absorption cross sections. The results agree with the previously determined relative cross sections[16] within 30%. Results are collected in Table 1. The concentration of C_2H_3F-HF complexes was estimated using the absolute absorption intensities of the ν_7 and ν_4 bands of matrix-isolated vinyl fluoride, whose intensity ratio is unchanged in the C_2H_3F-HF complex. The overall reaction balance (consumption of ethene and accumulation of the reaction products) for 16 K photolysis, where C_2H_3F-HF is the main product, obtained in this way is quite satisfactory (*vide infra*). The number of *trans*- and *gauche*-1,2-$C_2H_4F_2$ molecules, which are formed in secondary reactions upon 26 K photolysis or annealing and have shifted IR frequencies, was estimated using corresponding values for these molecules listed in Table 1.

DISCUSSION

A. IR Spectrum of the β-Fluoroethyl Radical. The observed correlations between the growth behavior of the two

4500 *J. Phys. Chem., Vol. 100, No. 11, 1996*

Misochko et al.

TABLE 2: Characteristics of Infrared Absorption Bands for β-Fluoroethyl Radical in Solid Argon

observed		calculated[a]		
ν, cm^{-1}	integrated absorption cross section B_i, km/mol[b]	assignment	ν, cm^{-1}	integrated absorption cross section B_i, km/mol[b]
		CH$_2$ stretch	3094	12.1
		CH$_2$ stretch	2997	5.3
2885	13.0 ± 2	C*H$_2$ stretch	2932	56.2
2856	17.6 ± 2	C*H$_2$ stretch	2879	57.1
		C*H$_2$ bend	1498	0.5
1449	6 ± 2	CH$_2$ bend + C*H$_2$ wag	1438	16.8
1426	9.5 ± 2.5	C*H$_2$ wag + CH$_2$ bend	1400	16.1
1242	1.5 ± 0.5	C*H$_2$ wag	1238	2.5
1139	38 ± 10	CF stretch	1110	47.6
1087	85 ± 25	C*C stretch + CF stretch	1070	58.5
		C*H$_2$ rock + C*C stretch	964	23.8
862	13.8 ± 3	CH$_2$ rock + C*H$_2$ rock	839	13.1
		C*CF bend + inversion	445	30.5
		CH$_2$ inversion	388	20.4
		torsion	161	1.7

[a] Ref 26. [b] Base e.

prominent broad features 1087 and 1139 cm^{-1} with the consumption of isolated ethene molecules and growth of the β-C$_2$H$_4$F radical from the EPR data I upon annealing (Figure 4) and photolysis at 26 K suggest assignment of these features to the β-fluoroethyl radical. Analysis of the spectra reveals other bands which appear upon annealing or 26 K photolysis with the same growth kinetics as the broad bands at 1087 and 1139 cm^{-1} and can be assigned to vibrational modes of the β-C$_2$H$_4$F radical. Results are presented in Table 2 along with recently calculated frequencies and absorption intensities.[26] The calculated frequencies agree with experimental ones within 5−50 cm^{-1}. Strong bands calculated to be at 964, 2997, and 3094 cm^{-1} are probably masked by the ethene absorptions in the samples.

Calculation of the mass balance between reactants and products permits the determination of absolute integrated absorption intensities of the β-fluoroethyl radical IR bands. Two different types of experiments were used for this purpose. Annealing of samples photolyzed at 16 K does not change concentrations of the closed-shell products (Figure 1B), whereas the bands corresponding to the radical increase by a factor of ~7. Growth of the intensity of these bands was compared with the decrease of the ethene concentration, whose absolute absorption intensities are given in Table 1. Balance of reactants and products upon photolysis at 26 K gives the absolute concentrations of the radicals in a similar way. In this case, the fraction of ethene molecules which forms C$_2$H$_4$F$_2$ and C$_2$H$_3$F−HF is taken into account. Both series of experiments give cross sections for the β-C$_2$H$_4$F radical which agree to within 25%. Table 2 lists absolute integrated absorption intensities of the observed IR bands averaged over four experiments (two of each type). It shows good agreement of both frequencies and intensities with the values calculated by Chen *et al.*[26] Three bands of this radical trapped in an Ar matrix were assigned earlier by Jacox[14] to be at 2860, 1047, and 427 cm^{-1}. The 2860 cm^{-1} band agrees with the 2856 cm^{-1} frequency measured in this study. The band at 1047 cm^{-1} in our experiments is unambiguously assigned to *trans*-difluoroethane, in agreement with the results of Hauge *et al.*,[15] Frei *et al.*[16] and IR matrix isolation spectra of this molecule.[21,22,25] The low-frequency

TABLE 3: Reaction Balance between Ethene Consumption and Formation of Products after 1.5 h Photolysis of Samples of Ar−F$_2$−CH$_4$ = 1000:1:1

temp, K	ethene consumption	formation of products[a]			
		C$_2$H$_3$F	*t*-C$_2$H$_4$F$_2$	*g*-C$_2$H$_4$F$_2$	C$_2$H$_4$F
16	6.2 ± 0.7	3.4 ± 0.4	1.2 ± 0.2	1.2 ± 0.2	0.8 ± 0.3
26	14.5 ± 2	3.8 ± 0.4	1.1 ± 0.2	1.3 ± 0.3	8.5 ± 2.5

[a] Percent reaction or product formation relative to the initial ethene concentration.

band 427 cm^{-1} is out of the range of our spectrometer but is in reasonable agreement with the 445 cm^{-1} frequency calculated by Chen *et al.*[26]

The assignment of the IR spectra in combination with EPR study shows that the photolysis of F$_2$ yields two types of products: β-C$_2$H$_4$F radicals and closed-shell products. Reaction yields for these two channels at 16 and 26 K are given in Table 3. At 26 K, the radical is the main product of photolysis. Reactions of thermal F atoms with β-C$_2$H$_4$F radicals at this temperature will be considered in section C below. At 16 K, formation of closed-shell products is dominating by far; the fraction of radicals in the products is ~0.1. The low radical yields at 16 K make it difficult to reliably establish the mechanism of formation (i.e., whether they arise from reaction of translationally hot F atoms with isolated C$_2$H$_4$ after long-range migration or by photolysis of F$_2$−C$_2$H$_4$ complexes and loss of F from the cage). However, the observed consumption of isolated C$_2$H$_4$ molecules in photolysis at 16 K (0.05−0.1 of the ethene concentration consumed in photolysis) approximately balances the production of radicals. This suggests that radicals produced at 16 K are formed by reaction of long-range migrating hot F atoms with isolated ethene molecules. The highest concentration of radicals formed in reaction of translationally hot F atoms with isolated C$_2$H$_4$ can be estimated using the formula[5] max[C$_2$H$_4$F]/[F$_2$] ~ σNL, where σ is the reaction cross section, L is thermalization length, and N and [F$_2$] are initial concentrations of isolated C$_2$H$_4$ and F$_2$ in the sample, respectively. At σ ~ 5 × 10^{-16} cm^2 and L ~ 100 Å, the fraction of radical product will be ~0.1. Thus, even when only 6% of the ethene is present as F$_2$−C$_2$H$_4$ complexes and the thermalization length is as large as 100 Å, the radicals formed by translationally hot F atoms combining with isolated C$_2$H$_4$ are difficult to detect by infrared spectroscopy.

B. UV Photolysis of Matrix-Isolated F$_2$−C$_2$H$_4$ Complexes. The photochemical kinetics at 16 K clearly show that the closed-shell products (C$_2$H$_3$F−HF and 1,2-difluoroethane) are formed by a one-photon absorption mechanism. This requires that both F atoms produced by photodissociation of the F$_2$ molecule react with the same C$_2$H$_4$ molecule. Molecular dynamics (MD) simulations of the photodissociation of the F$_2$ molecule isolated in crystalline Ar show that, in the event of cage escape of both hot F atoms, they move in the opposite directions and the probability that their trajectories cross is essentially zero.[3] Extensive photolysis at 16 K results in almost exclusive bleaching of ethene molecules in complexes with F$_2$ (Figure 1A). Taking into account the absence of diffusion at 16 K and the balance between consumption of the reactant complexes and product accumulation (Table 3), we conclude that formation of the closed-shell products occurs in reaction in the F$_2$−C$_2$H$_4$ complex, when neither of the photogenerated F atoms escapes from the cage. This means that the initial geometry of the complex and the surrounding Ar atoms significantly reduces the cage escape probability of the nascent F atoms compared to photodissociation of an isolated F$_2$ molecule.[1] In MD simulations,[3,4] an F$_2$ molecule in a singly substitutional Ar lattice site causes only slight perturbation of the lattice and rotates almost freely. As a result, both atoms escape from the parent

Reactions of Photogenerated F Atoms with Ethene

J. Phys. Chem., Vol. 100, No. 11, 1996 **4501**

cage through triangular lattice cage windows whenever the F_2 orientation lies within "reaction cones" defined by the lattice geometry and energetics.[3] Conversely, a $F_2-C_2H_4$ complex is likely to occupy a double substitutional site (or single substitutional and the nearest interstitial site), causing strong deformation of the lattice. This condition and bonding in the complex may diminish the size of the exit cones for the hot atoms.

The first step of the cage reaction in the $F_2-C_2H_4$ complex is formation of two F atoms with a total of ∼2 eV excess energy. The closed-shell products must be formed by successive addition of these atoms to C_2H_4. The primary reaction of one F atom with C_2H_4 produces an excited intermediate $C_2H_4F^*$:

$$[F + F + C_2H_4] \rightarrow [F + C_2H_4F^*] \qquad (4)$$
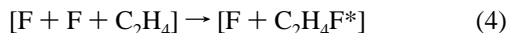
The next reaction step is most likely recombination of this intermediate with the second F atom, leading to formation of a highly vibrationally excited adduct $C_2H_4F_2^*$. From the results of Frei *et al.*[16,17] and the MD simulation of Raff,[27,28] it follows that $C_2H_4F_2^*$ in the rare gas matrix can undergo vibrational relaxation to *trans*- or *gauche*-difluoroethane or undergo elimination to C_2H_3F and HF:

$$[C_2H_4F_2^*] \rightarrow [C_2H_3 + HF] \ (p_1 \simeq 0.6) \qquad (5a)$$

$$\rightarrow [trans\text{-}C_2H_4F_2] \ (p_2 \simeq 0.2) \qquad (5b)$$

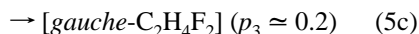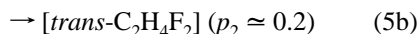$$\rightarrow [gauche\text{-}C_2H_4F_2] \ (p_3 \simeq 0.2) \qquad (5c)$$

Figure 3 demonstrates that these products are formed in direct competition (single-exponential kinetics with the same characteristic time). The relative yields of the channels represented by reactions 5 are calculated from the overall yields shown in Table 3.

A possible alternative mechanism for C_2H_3F-HF formation is decomposition of the primary intermediate $C_2H_4F^*$ into C_2H_3F and an H atom (similar to the gas phase process[8]); the latter subsequently recombines with the second F atom. The characteristic time of H atom elimination from $C_2H_4F^*$ in the gas phase is of the order of 1 ns, and there is no reason to believe that it is shorter in the solid. Thus, this mechanism may be significant only if the second F atom does not recombine with the radical on the time scale of 1 ns.

In the gas phase, decomposition of the excited $C_2H_4F_2^*$ has unit probability.[13,28] In rare gas crystals, however, MD simulations[27,28] gave high vibrational relaxation rates for the molecule in an interstitial or substitutional site of the fcc argon lattice. The calculated product ratio $[C_2H_3F-HF]/[C_2H_4F_2]$ is less than unity and is significantly lower than the experimental values measured by Frei *et al.*,[16] as well as in the present work. This disagreement was suggested to be caused by the difference in the lattice cage geometry used in the calculation compared with the real experimental systems.

C. Reactions of Thermalized F Atoms. Comparison of the IR and EPR experiments shows that the main product of the reaction of C_2H_4 with thermal F atoms diffusing at 20−26 K is the β-fluoroethyl radical (reaction 1). Recombination of diffusing F atoms with C_2H_4F radicals forms the secondary products

$$C_2H_4F + F \rightarrow (trans \ or \ gauche)\text{-}1,2\text{-}C_2H_4F_2 \qquad (6)$$
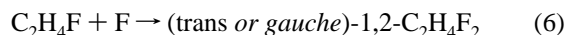
The measured kinetics of $1,2\text{-}C_2H_4F_2$ formation via secondary reaction of diffusing F atoms permits us to determine the ratio of rate constants k_1/k_6 for reactions 1 and 6. Assuming a quasistationary concentration of F atoms during photolysis, at the initial stage (when $k_1[C_2H_4] \gg k_6[C_2H_4F]$) the yield of the
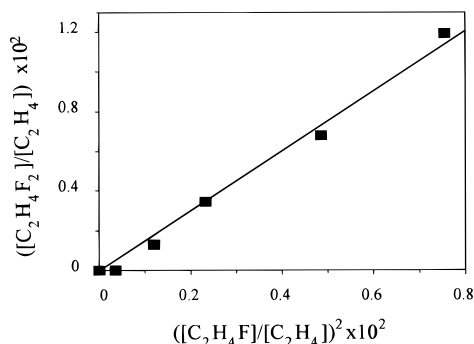
Figure 7. Dependence of the secondary product concentration (1053.2 cm^{-1} band) on the concentration of the radicals.

secondary product $C_2 = [C_2H_4F_2]/[C_2H_4]$ depends quadratically on the yield of the radical $C_1 = [C_2H_4F]/[C_2H_4]$:

$$C_2 = (k_6/2k_1)C_1^2$$

This dependence is presented in Figure 7. The ratio (determined from the slope of the plot) is $k_1/k_6 = 0.3 \pm 0.1$; the uncertainty is determined by the accuracy of the absolute concentration measurements.

The branching (5) between HF elimination (formation of the C_2H_3F-HF complex) and stabilization of $C_2H_4F_2$ is drastically different in the photoinduced reaction in the $F_2-C_2H_4$ complex from that in the thermal reaction (6). In the former, the elimination channel is favorable. In the latter, the formation of C_2H_3F-HF is not observed, and only the conformers of difluoroethane are stabilized. This difference may be qualitatively explained by considering the branching a result of competition between vibrational relaxation of the energy-enriched adduct $(C_2H_4F_2)^*$ and the elimination reaction. There are two factors which can affect this competition: (a) $(C_2H_4F_2)^*$ is formed in cages of different size; (b) $(C_2H_4F_2)^*$ is formed with different excess energies.

The $F_2-C_2H_4$ complex is likely to occupy a larger lattice site than a single isolated ethene molecule. Thus, the reaction in complex forms $(C_2H_4F_2)^*$ in a more spacious cage than reaction 6. This conclusion is supported by the observed blue shift of the IR bands of the difluoroethane formed via (6) compared to that formed by UV photolysis of $F_2-C_2H_4$ complexes. Additional support for this conclusion comes from the fact that a higher temperature is required for the *trans−gauche* interconversion of the $C_2H_4F_2$ formed in the tighter lattice site. According to the aforementioned MD calculations,[28] and a more recent study of the effects of matrix morphology on the dynamics of $F_2-C_2H_4$ photolysis reaction,[29] a larger cage leads to a lower relaxation rate and therefore favors the formation of the elimination product C_2H_3F-HF. Formation of difluoroethane from reaction 6, on the other hand, probably occurs in a smaller cage site. Stronger matrix−guest interactions due to the size mismatch of this product lead to much faster relaxation of the intermediate, thereby reducing the importance of the HF elimination channel.

In reaction of the complex, space for the HF elimination product molecule is reserved by F_2; i.e., reactants $C_2H_4-F_2$ and product C_2H_3F-HF likely have similar sizes. Thus, little rearrangement of the surrounding cage is required. In reaction 6, where both F atoms come from the bulk, failure to form the elimination product (C_2H_3F-HF) may be partly due to the inability of the lattice cage to expand to accommodate its larger size compared with C_2H_4.

The enthalpy of reaction 6 is $\Delta H = -427$ kJ/mol, so that the product $C_2H_4F_2$ is formed with high vibrational excess energy. The energy of the same product formed in the UV-
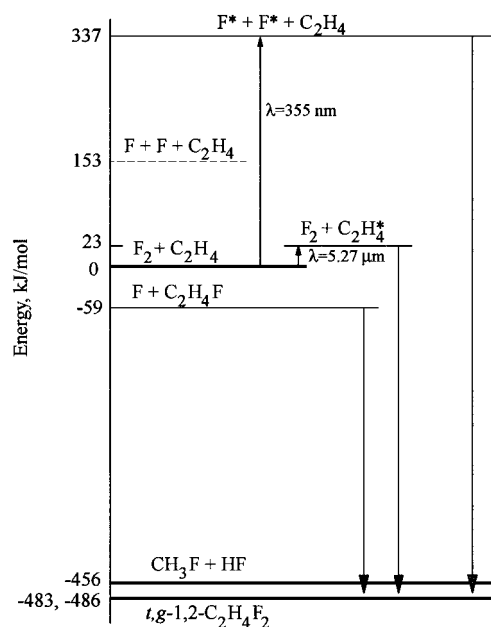
Figure 8. Energy diagram of the reactants, intermediates, and products in the system $F_2 + C_2H_4$.

initiated cage reaction of the complex $F_2-C_2H_4$ can be as much as 400 kJ/mol higher, depending on the relative rates of atomic addition and energy transfer from the excited intermediates of (4) to the matrix (see Figure 8). This also can explain the predominant formation of the elimination product in the reaction sequence (4−5). The energy diagram in Figure 8 also shows the initial energy of the $C_2H_4F_2^*$ formed in the $F_2-C_2H_4$ complex by IR excitation at $\lambda = 5.27\ \mu$m, studied by Frei *et al.*[16] In spite of the large difference in the available excess energies in IR- and UV-induced reactions, the elimination channel (5a) is predominant in both cases. On the other hand, the excess energy in the IR-induced reaction of the complex (508 kJ/mol) is close to that in the thermal reaction (6), which produces exclusively $C_2H_4F_2$ molecules. This implies that the energy factor is less important than the effect of the cage size in competition between relaxation and elimination in reactions 5.

As demonstrated above, the observed difference in products of reactions 5 and 6 clearly shows that decomposition of highly excited intermediates is predominant when the reactants are initially arranged as complexes. In particular, this can play an important role in aggregates of several reactant molecules or in their binary mixtures, leading to specific chain reactions propagated by the decomposition products. The possibility of such a two-step energetic chain in $(F_2\cdots CH_4\cdots F_2)$ was recently demonstrated.[30]

CONCLUSIONS

(1) The combination of kinetic IR and EPR data in experiments at different temperatures allows assignment of the vibrational bands of the β-fluoroethyl radical. Absolute absorption intensities of eight vibrational modes have been measured.

(2) Closed-shell products are formed when reactants are initially arranged as $F_2-C_2H_4$ complexes. The geometry of the complex and surrounding Ar atoms is such that neither of the F atoms formed by photodissociation of F_2 escapes from the cage. Closed-shell products C_2H_3F-HF complex and *trans*- and *gauche*-1,2-$C_2H_4F_2$ are formed with the relative yields 0.6: 0.2:0.2.

(3) The main product of reaction of F atoms (either hot or thermalized) with isolated C_2H_4 molecules is the β-fluoroethyl radical. In the absence of F atom diffusion, the fraction of radicals in the product balance is about 0.1. However, at $T > 20$ K, reactions of diffusing thermal F atoms form C_2H_4F radicals as the major product.

(4) Secondary reaction of a thermal F atom with the β-C_2H_4F radical forms *trans*- and *gauche*-1,2-$C_2H_4F_2$ but not C_2H_3F-HF. The rate constant of this radical recombination reaction is about 3 times larger than the rate constant of the primary F + C_2H_4 reaction at 26 K.

(5) The difference between products of the UV photolysis reaction of $F_2-C_2H_4$ complexes and reaction of two thermalized F atoms with isolated C_2H_4 is explained by the difference in size of the reaction cages and excess energies of the vibrationally excited intermediate $(C_2H_4F_2)^*$.

References and Notes

(1) Feld, J.; Kunttu, H.; Apkarian, V. A. *J. Chem. Phys.* **1990**, *93*, 1009.
(2) Kunttu, H.; Apkarian, V. A. *Chem. Phys. Lett.* **1990**, *171*, 423.
(3) Alimi, R; Gerber, R. B.; Apkarian, V. A. *J. Chem. Phys.* **1990**, *92*, 3551.
(4) Alimi, R.; Gerber, R. B.; Apkarian, V. A. *Phys. Rev. Lett.* **1991**, *66*, 1295.
(5) Misochko, E. Ya.; Benderskii, V. A.; Goldschleger, A. U.; Akimov, A. V. *Mendeleev Commun.* **1995**, *5*, 198.
(6) Misochko, E. Ya.; Benderskii, V. A.; Goldschleger, A. U.; Akimov, A. V.; Shestakov, A. F. *J. Am. Chem. Soc.*, submitted for publication.
(7) Benderskii, V. A.; Goldschleger, A. U.; Akimov, A. V.; Misochko, E. Ya.; Wight, C. A. *Mendeleev Commun.* **1995**, *6*, 245.
(8) Parson, J. M.; Lee, Y. T. *J. Chem. Phys.* **1972**, *56*, 4658.
(9) Moehlmann, J. G.; Gleaves, J. T.; Hudgen, J. W.; McDonald, J. D. *J. Chem. Phys.* **1974**, *60*, 4790.
(10) Farrar, J. M.; Lee, Y. T. *J. Chem. Phys.* **1976**, *65*, 1414.
(11) Bauer, S. H. *Chem. Rev.* **1978**, *28*, 147.
(12) Kato, S.; Morokuma, K. *J. Chem. Phys.* **1980**, *72*, 206.
(13) Kapralova, G. A.; Chaikin, A. M.; Shilov, A. E. *Kinet. Katal.* **1967**, *8*, 485.
(14) Jacox, M. E. *Chem. Phys.* **1981**, *58*, 289.
(15) Hauge, R. H.; Gransden, S.; Wang, J.; Margrave, J. L. *Ber. Bunsen-Ges. Phys. Chem.* **1978**, *82*, 104; *J. Am. Chem. Soc.* **1979**, *101*, 6950.
(16) Frei, H.; Fredin, L.; Pimentel, G. C. *J. Chem. Phys.* **1981**, *74*, 397.
(17) Frei, H.; Fredin, L.; Pimentel, G. C. *J. Chem. Phys.* **1983**, *78*, 3698.
(18) Misochko, E. Ya.; Benderskii, V. A.; Goldschleger, A. U.; Akimov, A. V. *Mendeleev Commun.* **1994**, *5*, 203.
(19) Johnson, G. L.; Andrews, L. *J. Am. Chem. Soc.* **1982**, *104*, 3043.
(20) Anderson, D. T.; Winn, J. S. *Chem. Phys.* **1994**, *189*, 171.
(21) Huber-Wälchli, P.; Günthard, Hs. H. *Chem. Phys. Lett.* **1975**, *30*, 347.
(22) Harris, W. C.; Holtzclaw, J. R.; Kalasinsky, V. F. *J. Chem. Phys.* **1977**, *67*, 3330.
(23) Fredin, L.; Nelander, B. *J. Mol. Struct.* **1973**, *16*, 205.
(24) Wight, C. A.; Misochko, E. Ya.; Vetoshkin, E. V.; Goldanskii, V. I. *Chem. Phys.* **1993**, *170*, 393.
(25) Dubs, M.; Ermanni, L.; Günthard, Hs. H. *J. Mol. Spectrosc.* **1982**, *91*, 458.
(26) Chen, Y.; Rauk, A.; Tschuikow-Roux, E. *J. Chem. Phys.* **1990**, *93*, 6620.
(27) Raff, L. M. *J. Chem. Phys.* **1990**, *93*, 3160 and references therein.
(28) Raff, L. M. *J. Chem. Phys.* **1990**, *93*, 3160; **1991**, *95*, 8901.
(29) Raff, L. M. *J. Chem. Phys.* **1992**, *97*, 7459.
(30) Misochko, E. Ya.; Benderskii, V. A.; Goldschleger, A. U. *J. Phys. Chem.* **1995**, *99*, 13917.

JP953155F